ISSN 2072-5981
doi: 10.26907/mrsej

Magnetic Resonance in Solids

Electronic Journal

Volume ***21***
Special Issue 3
Paper No ***19306***
1-8 pages
2019
doi: **10.26907/mrsej-19306**

http://mrsej.kpfu.ru
http://mrsej.ksu.ru

Established and published by Kazan University
Endorsed by International Society of Magnetic Resonance (ISMAR)
Registered by Russian Federation Committee on Press (#015140),
August 2, 1996
First Issue appeared on July 25, 1997

"***Magnetic Resonance in Solids. Electronic Journal***" (**MRSej**) is a peer-reviewed, all electronic journal, publishing articles which meet the highest standards of scientific quality in the field of basic research of a magnetic resonance in solids and related phenomena.

Indexed and abstracted by
Web of Science (*ESCI*, Clarivate Analytics, from 2015),
Scopus (Elsevier, from 2012), *RusIndexSC* (*eLibrary*, from 2006), *Google Scholar*,
DOAJ, *ROAD*, *CyberLeninka* (from 2006), *SCImago Journal & Country Rank*, etc.

---

* In Kazan University the Electron Paramagnetic Resonance (EPR) was discovered by Zavoisky E.K. in 1944.

Short cite this: *Magn. Reson. Solids* **21**, 19306 (2019) doi: 10.26907/mrsej-19306

Intrinsic spin resonance in iron pnictides

H.-A. Krug von Nidda*, M. Hemmida, S. Kraus, N. Pascher, J. Deisenhofer, A. Loidl
Experimentalphysik V, Center for Electronic Correlations and Magnetism,
Institute for Physics, University of Augsburg, D-86135 Augsburg, Germany
**E-mail: kvn@physik.uni-augsburg.de*

(Received April 11, 2019; accepted April 12, 2019; published April 19, 2019)

We report on ESR measurements in polycrystalline LaFeAsO and PrFeSbO and in single crystalline Mn-doped $Ba(Fe_{0.975}Mn_{0.025})_2As_2$. The absorption spectrum can be described by a broad resonance line with Lorentzian lineshape. The intensity of the resonance absorption follows the temperature dependence of the dc-susceptibility and mirrors the spin-density wave anomaly, while the linewidth roughly agrees with the electrical resistivity.

PACS: 76.30.-v, 76.30.Fc, 76.30.Pk.
Keywords: iron based superconductors, electron spin resonance.

In honor of Professor Boris Ivanovich Kochelaev

Preface

Exactly 25 years ago, the first common paper of Prof. Boris I. Kochelaev and our research team, which at that time still worked at the Technical University Darmstadt, was published entitled "Spin dynamics in $La_{2-x}Sr_xCuO_{4+\delta}$ doped with Mn as revealed by an ESR study" [1]. This was the starting point of a very fruitful collaboration on electron spin resonance in high-T_c cuprates. Here Prof. Kochelaev's explanation of the intrinsic ESR signal in $La_{2-x}Sr_xCuO_4$ to result from three-spin polarons in the copper-oxide planes is of invaluable importance [2]. Further highlights of our continued collaboration on ESR in strongly correlated electron systems to be mentioned are the characterization of orbital order from the anisotropy of the ESR linewidth in manganites and the explanation of the magnetic resonance in the heavy-fermion compound $YbRh_2Si_2$. Now on occasion of Prof. Kochelaev's 85th birthday, we return to a topic of unconventional superconductivity and discuss so far unpublished results of intrinsic ESR signals in iron pnictides.

1. Introduction

The discovery of superconductivity in "1111" LaFeAsO is reported, for first time, in 2006 [3]. Although in that work the transition temperature was low ($T_c = 3.5\,K$), a rapid progress showed up already in February 2008, as Kamihara *et al.* found superconductivity with $T_c = 26\,K$ in the fluorine-doped compound $LaFeAsO_{1-x}F_x$ [4]. The mother compound LaFeAsO is an antiferromagnetic metal in which on cooling magnetic ordering of the itinerant iron spins in terms of a spin-density wave sets in at a transition temperature of about $T_{SDW} \approx 140\,K$ accompanied by a structural phase transition from a tetragonal into an orthorhombic phase. On substituting oxygen with fluorine, T_{SDW} significantly decreases as the fluorine concentration increases. At $x \approx 0.1$, long-range magnetic order disappears and a superconducting state sets in. A typical phase diagram of this type of compounds is shown in Ref. [5]. This phase diagram resembles that one which has been found in high-T_c copper oxide superconductors like $(La_{1-x}Sr_x)_2CuO_4$ [6].

In both copper oxide and iron-based superconductors, doping induces charge carriers (electrons or holes) which suppress the antiferromagnetic ordering and lead to the formation of Cooper pairs. The closeness of T_c to the magnetic transition suggests that the observed high T_c values are due to a carrier pairing mechanism supported by spin fluctuations. This is confirmed e.g. by findings in thin films of the electron-doped copper oxide $La_{2-x}Ce_xCuO_4$, where electron pairing is linked to spin fluctuations; i.e. the linear dependence on temperature of the resistivity is caused by spin-fluctuation scattering [7]. Furthermore, FeAs-based systems are built up from FeAs planes, intermediated by LaO layers. This is analogous to cuprates where the stacked CuO_2 planes are separated by the La- or Y-Ba layers. Due to of their layered structure, both types of systems are strongly anisotropic, and reveal quasi two-dimensional electronic states [8].

The "122" mother compound $BaFe_2As_2$ serves as another starting point in searching for high-T_c superconductivity in iron pnichtides [9]. Similar to LaFeAsO, the system undergoes a structural phase transition from tetragonal into orthorhombic phase at 140 K, where the structural transition is accompanied by formation of a spin-density wave of the iron spins. Doping enhances the quasi two-dimensional electronic properties in $BaFe_2As_2$ and leads to superconductivity, obviously involving magnetic excitations. For example, neutron scattering studies in $BaFe_{1.84}Co_{0.16}As_2$ exhibit that this compound turned out to be more quasi-two-dimensional than stoichiometric $BaFe_2As_2$ [10]. On cooling below T_c, a clear resonance peak is observed at a wave vector with an energy of 8.6 meV, corresponding to $4.5k_BT_c$. This was in good agreement with the canonical value of $5k_BT_c$ observed in cuprates. In the Ni-doped compound $BaFe_{1.96}Ni_{0.04}As_2$ the separation of structural and magnetic transition was investigated in detail. While in the undoped state, $BaFe_2As_2$ exhibits simultaneous structural and magnetic phase transitions at 143 K, electron doped $BaFe_{1.96}Ni_{0.04}As_2$ first displays the lattice distortion near 97 K, and then orders antiferromagnetically at 91 K before developing weak superconductivity around 15 K [11]. These results indicate that the transition from three-dimensional spin waves to quasi-two-dimensional spin excitations by electron doping is important for the separated structural and magnetic phase transitions in iron arsenides, i.e. as a result of weakening of the magnetic exchange interaction between the FeAs-layers. Moreover, the two-dimensional character is obviously important for superconductivity.

The coexistence of superconductivity and magnetism in these types of compounds motivates the application of magnetic resonance techniques in order to use the electron spins as local probe to access the microscopic mechanism of superconductivity. So far several electron spin resonance (ESR) studies have been performed on Gd-based "1111" [12,13] and Eu-based "122" iron pnictides [14–20], making use of the stable magnetic moment of the rare-earth ions Gd^{3+} and Eu^{2+} both containing a half-filled $4f$ shell with spin $S = 7/2$. Here we report ESR measurements in polycrystalline LaFeAsO and PrFeSbO and in single crystalline Mn-doped $BaFe_2As_2$ ($BaFe_{1.95}Mn_{0.05}As_2$) which indicate the existence of very broad intrinsic spin resonance signals from the itinerant iron spin system.

2. Experimental details

Polycrystalline samples of $LaFeAsO_{1-x}F_x$ ($x = 0, 0.1$) and PrFeSbO were prepared following the procedure described in Ref. [21]. Powder x-ray diffraction measurements confirmed that the structure is tetragonal of ZrCuSiAs-type, with lattice parameters consistent with previous reports [22, 23]. $Ba(Fe_{1-x}Mn_x)_2As_2$ ($x = 2.5\%$, 5% and 12%) single crystals of $ThCr_2Si_2$ structure were grown from self-flux in zirconia crucibles sealed in quartz ampoules under argon atmosphere, as described in Ref. [24].

ESR measurements were performed in a Bruker ELEXSYS E500 CW-spectrometer at X- and Q-band frequencies ($\nu \approx 9.4$ GHz and 34 GHz, respectively) equipped with a continuous helium gas-flow cryostat working in the temperature region $4 < T < 300$ K. The polycrystalline sample were powdered and placed into quartz tubes which were sealed in He atmosphere. ESR detects the power P absorbed by the sample from the transverse magnetic microwave field as a function of the static magnetic field H. The signal-to-noise ratio of the spectra is improved by recording the derivative dP/dH using lock-in technique with field modulation.

3. Results and discussion

1111 Compounds

In Fig. 1a we show typical ESR spectra of LaFeAsO for different temperatures. The overall shape of the absorption is determined by an extremely broad line, which seems to have a resonance field close to zero. On top of this absorption feature a second much weaker resonance signal is visible at a resonance field of approximately $H_{\mathrm{res}} \sim 3\,\mathrm{kOe}$. To separate these two contributions we fitted the absorption spectra with two Lorentzians also accounting for contributions at reversed magnetic field as described in Ref. [25]. Given the fact that the main resonance is of the "bath-tub" shape, one has to perform this analysis with great care. Astonishingly, the fitting procedure proved to be very stable and we reduced the number of fit parameters by fixing the resonance field of the broad line equal to zero, since the fit always converged to this value. The fits describe the observed absorption spectra nicely and we plot the temperature dependences of the resulting fit parameters in Fig. 1(b-d).

Fig. 1b compares the double integrated intensities of both lines. The intensity of the broad line, which is normalized to unity at room temperature, monotonously decreases on decreasing temperature with a kink clode to T_{SDW} followed by a stronger decrease. The intensity of the second line is about 0.2% of the main line at room temperature but increases on decreasing temperature up to about 7% at 50 K. At lower temperature a separation of the two lines is not reasonable anymore, because the weak line becomes too broad to be discernible. Therefore the anomaly at 50 K obviously does not have any physical meaning. Note also that for $T = 4\,\mathrm{K}$ the anomalies visible on the spectrum at 3.4 kOe and 12 kOe result from the background of the cavity.

Fig. 1c shows the temperature dependence of the resonance field of the weak line which shifts from more than 3 kOe at room temperature down to about 1.6 kOe at 50 K. At the same time the corresponding linewidth depicted in the lower frame increases from 1 kOe to 3 kOe, respectively.

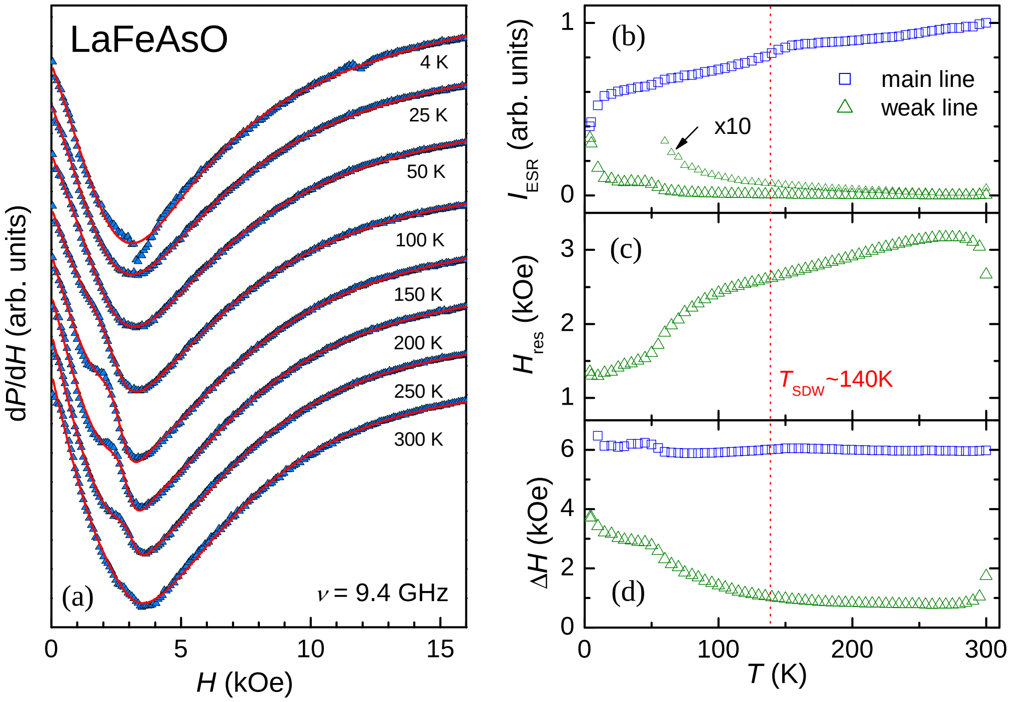

Figure 1. (a) ESR spectra of LaFeAsO taken at different temperatures between liquid-helium and room temperature. The solid line indicates a fit by two Lorentz lines as described in the text. Temperature dependence of (b) the ESR intensity I_{ESR}, (c) the resonance field H_{res}, and (d) the ESR linewidth ΔH of the two absorption lines in LaFeAsO.

Again the data at lower temperature will not be considered further. The linewidth of the broad line remains at about 6 kOe in the whole temperature range under investigation.

For further discussion we focus on the behavior of intensity and linewidth of the main resonance line on passing the spin-density wave transition as illustrated in Fig. 2. The ESR intensity nicely corresponds to the static susceptibility. Both quantities exhibit a gradual drop of about 20% below the SDW transition. At the same time the linewidth shows a comparable behaviour like the electrical resistivity as expected from the Elliot-Yafet theory [26, 27]. Thus, both the intensity and linewidth are indicative of the itinerant iron spin system as the origin of the resonance signal, i.e. we observe some kind of conduction electron spin resonance (CESR).

Usually the direct observation of CESR is only possible in very clean metals at very low temperatures or in low dimensional conductors. The latter situation seems to be realized in the iron pnictides, where the conductivity is significantly larger parallel to the FeAs planes than perpendicular to them. Indeed, the purity of the sample also plays an important role for the observability of the CESR signal, because already small amounts of paramagnetic impurities can mask the broad line. That is why only signals of localized spins have been reported in LaFeAsO so far. In our samples these localized spins give rise to the weak line which shows the Curie-Weiss like temperature dependence of the intensity reported earlier by Wu and coworkers [28]. Resonance field and linewidth of the weak line are of comparable magnitude as in that publication, where its absolute intensity was so strong that the coexistent broad resonance line was interpreted as tiny background of a secondary phase.

The problem with the defect signals became more severe for fluorine doped LaFeAsO$_{1-x}$F$_x$, where we were not able to reasonably separate the CESR line from the impurity line. Therefore, to date it was not possible to follow the resonance signal of the conduction electrons through the superconducting transition. Nevertheless, in the related compound PrSbFeO we detected a comparable broad ESR signal with similar properties as illustrated in Fig. 3. Starting with Fig. 3a, one can recognize the broad line centered at zero field for X-band frequency. At Q-band frequency (Fig. 3b) the ESR signal becomes fully visible as its resonance field shifts considerably away from zero. Again the X-band signal was fitted by a Lorentzian profile with the resonance field fixed at $H_{\mathrm{res}} = 0$. Like in LaFeAsO the intensity shown in Fig. 3c decreases monotonously on decreasing temperature by about 20% between room temperature and helium temperature.

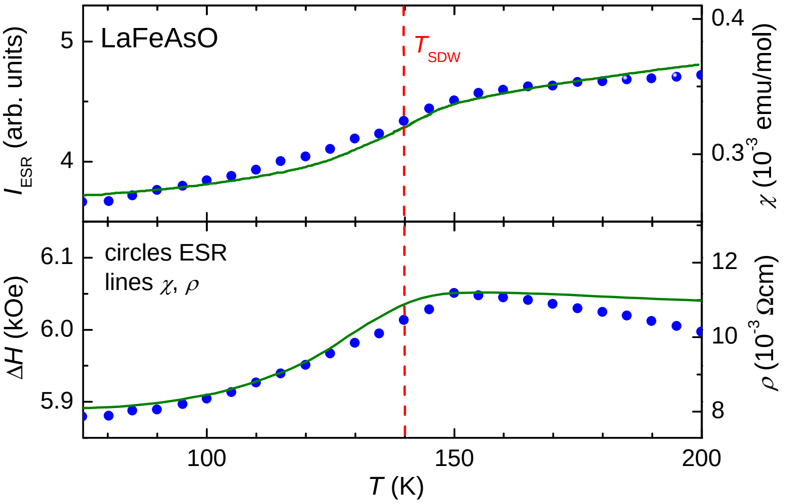

Figure 2. Temperature dependence of the ESR linewidth ΔH (upper frame), and intensity I_{ESR} (lower frame) in LaFeAsO compared to electrical resistivity and magnetic susceptibility (given as solid lines), respectively.

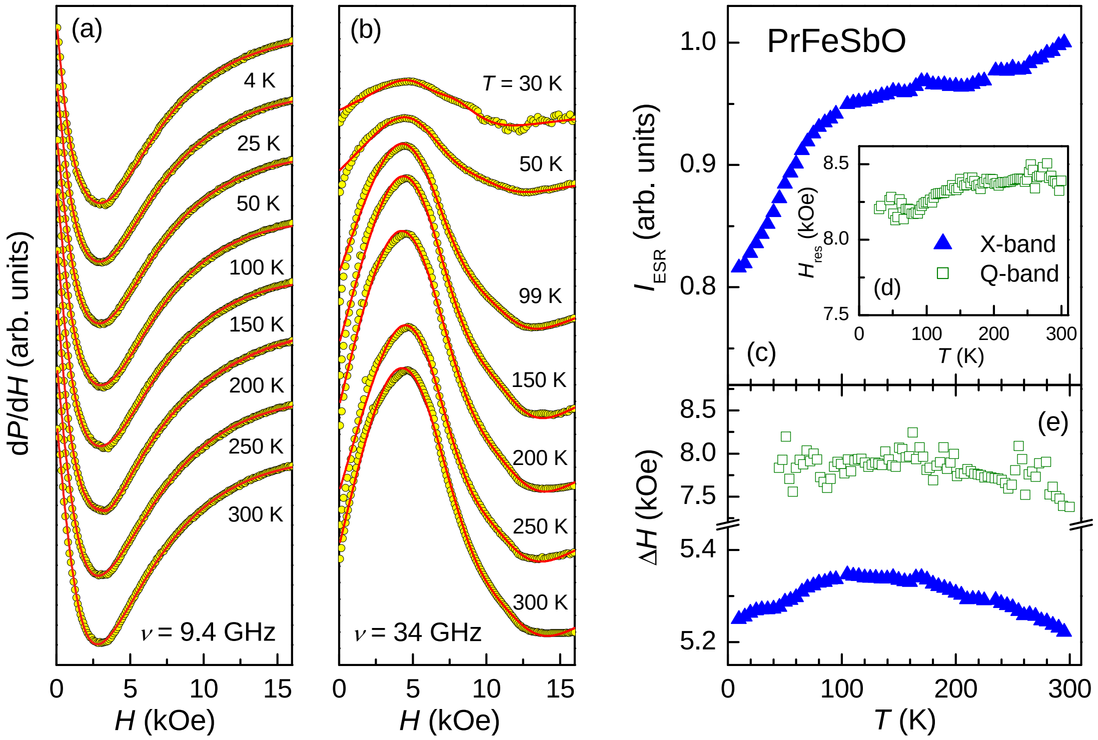

Figure 3. ESR spectra of PrFeSbO taken at different temperatures between liquid-helium and room temperature for X-Band (a) and Q-Band (b) frequencies, respectively. The solid line indicates a fit by two Lorentz lines as described in the text. Temperature dependence of (c) the ESR intensity I_{ESR} at X-band frequency, (d) resonance field H_{res} at Q-band frequency and (e) linewidth ΔH of the main line in PrFeAsO.

Below 100 K the slope is approximately 6 times higher than above. The linewidth is only weakly temperature dependent with a maximum value of about 5.3 kOe close to 100 K. At Q-band frequency, the resonance field was used as free parameter, resulting in only weakly temperature dependent resonance field $H_{\mathrm{res}} \sim 8.3$ kOe (Fig. 3d) and linewidth $\Delta H \sim 7.6$ kOe (Fig. 3e). Due to the huge linewidth the uncertainty of the resonance field does not allow to derive a reliable g value. Nevertheless, the non-zero resonance field proves the real magnetic resonance character of the observed absorption signal. The intensity is not a reliable quantity at Q-band frequency and not shown in Fig. 3c, because the quality factor of the cavity, which is cooled together with the sample, strongly depends on temperature. At X-band frequency the intensity can be evaluated, because the cavity is always kept on room temperature, while only the sample is cooled in the helium gas-flow cryostat.

At the moment not much additional information exists about the electric and magnetic properties of PrFeSbO. A direct comparison with the dc-susceptibility is not feasible due to the paramagnetic contribution of the Pr ions which masks the static susceptibility of the conduction electrons. Comparison of ESR intensity and linewidth with the corresponding data in LaFeAsO suggests a spin-density wave transition slightly below 100 K.

122 Compounds

In search for further indications of CESR in iron pnictides we discovered analogous absorption signals in single crystals of Mn doped $\mathrm{BaFe_2As_2}$ as shown in Fig. 4a. In the series under investigation Mn concentrations of 0, 2.5, 5 and 11.5 percent manganese have been available. The CESR signal was best observable in $\mathrm{Ba(Fe_{0.975}Mn_{0.025})_2As_2}$. Regarding the susceptibility of $\mathrm{Ba(Fe_{1-x}Mn_x)_2As_2}$ the sample with $x = 0.025$ exhibits the smallest residual susceptibility below

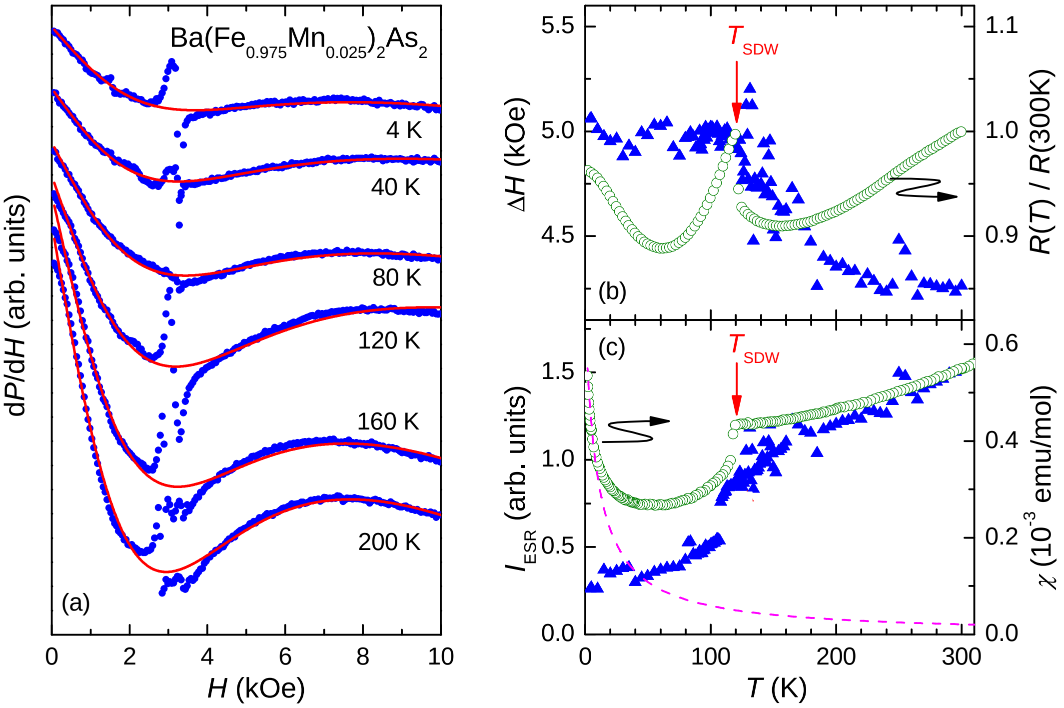

Figure 4. (a) ESR spectra of Ba(Fe:Mn)$_2$As$_2$ taken at different temperatures between liquid-helium and room temperature. Solid lines indicate fits by a Lorentz line. Temperature dependence of (b) the ESR intensity I_{ESR}, and (c) linewidth ΔH in Ba(Fe:Mn)$_2$As$_2$ compared to magnetic susceptibility and electrical resistivity (solid lines), respectively. The dashed line indicates a Curie-Weiss law.

the spin-density wave transition, i.e. even below the pure sample $x = 0$. This seems similar to the case of Mn doped FeSe$_{0.5}$Te$_{0.5}$ [29], where small amounts of manganese improve the quality of the crystal, possibly by reducing the amount of ferromagnetic inclusions like magnetite Fe$_3$O$_4$.

Again, as one can see in Fig. 4b, the intensity of the rather broad line nicely resembles the static susceptibility, except for low temperatures, where the Mn doping gives rise to a Curie-Weiss law of localized spins indicated as dashed line, which is certainly not visible in the CESR intensity. Also the relative changes of the linewidth depicted in Fig. 4c are comparable to the variation of the electrical resistance. Only the increase of the resistivity to high temperatures is not reproduced by the linewidth. But this is still in agreement with the generalized Elliott-Yafet theory which in case of spin transfer to neighboring bands and large electron-phonon coupling results in a stronger relative increase of the resistance as compared to the ESR linewidth, if the energy difference to the conduction band corresponds to the electronic relaxation rate, like e.g. observed in MgB$_2$ [30].

4. Summary

To summarize we identified three independent iron pnictides with detectable intrinsic electron spin resonance signals, as there are the 1111 compounds LaFeAsO and PrFeSbO, as well as the 122 compound BaFe$_2$As$_2$ doped with 2.5% Mn on the Fe site. In all cases the resonance lines are extremely broad with linewidths of $\Delta H > 5$ kOe and, therefore, do not possess any well defined resonance field. Nevertheless, the ESR intensity well agrees with the spin susceptibility of the conduction-electron system forming a spin-density wave on lowering the temperature. At the same time the temperature dependence of the linewidth satisfactorily agrees with the behavior of the electrical resistivity indicating the same relaxation channel for both quantities. These properties identify the itinerant electrons as the source of the observed ESR signals.

Acknowledgments

We are grateful to J.S. Kim, A.A. Haghighirad, Y. Liu, and G. Friemel for sample preparation, crystal growth, and resistivity data. We thank Dana Vieweg for the SQUID measurements. We acknowledge financial support by the Deutsche Forschungsgemeinschaft (DFG, German Research Foundation) – Projektnummer 107745057 – TRR 80 "From Electronic Correlations to Functionality" (Augsburg, Munich, Stuttgart).

References

1. Kochelaev B.I., Kan L., Elschner B., Elschner S. *Phys. Rev. B* **49**, 13106 (1994)
2. Kochelaev B.I., Sichelschmidt J., Elschner B., Lemor W., Loidl A. *Phys. Rev. Lett.* **79**, 4274 (1997)
3. Kamihara Y., Hiramatsu H., Hirano M., Kawamura R., Yanagi H., Kamiya T., Hosono H. *J. Am. Chem. Soc.* **128**, 10012 (2006)
4. Kamihara Y., Watanabe T., Hirano M., Hosono H. *J. Am. Chem. Soc.* **130**, 3296 (2008)
5. Zhao J., Huang Q., de la Cruz C., Li S., Lynn J.W., Chen Y., Green M.A., Chen G.F., Li G., Li Z., Luo J.L., Wang N.L., Dai P. *Nat. Mater.* **7**, 953 (2008)
6. Varma C. *Nature* **468**, 184 (2010)
7. Jin K., Butch N.P., Kirshenbaum K., Paglione J., Greene R.L. *Nature* **476**, 73 (2011)
8. Izyumov Yu., Kurmaev E. *High-T_c Superconductors Based on FeAs Compounds*, Springer Series in Material Science, Vol. 143, Springer-Verlag, Berlin-Heidelberg (2010)
9. Rotter M., Tegel M., Johrendt D. *Phys. Rev. Lett.* **101**, 107006 (2008)
10. Lumsden M.D., Christianson A.D., Parshall D., Stone M.B., Nagler S.E., MacDougall G.J., Mook H.A., Lokshin K., Egami T., Abernathy D.L., Goremychkin E.A., Osborn R., McGuire M.A., Sefat A.S., Jin R., Sales B.C., Mandrus D. *Phys. Rev. Lett.* **102**, 107005 (2009)
11. Harriger L.W., Schneidewind A., Li S., Zhao J., Li Z., Lu W., Dong X., Zhou F., Zhao Z., Hu J., Dai P. *Phys. Rev. Lett.* **103**, 087005 (2009)
12. Alfonsov A., Muranyi F., Kataev V., Lang G., Leps N., Wang L., Klingeler R., Kondrat A., Hess C., Wurmehl S., Köhler A., Behr G., Hampel S., Deutschmann M., Katrych S., Zhigadlo N.D., Bukowski Z., Karpinski J., Büchner B. *Phys. Rev. B* **83**, 094526 (2011)
13. Alfonsov A., Muranyi F., Leps N., Klingeler R., Kondrat A., Hess C., Wurmehl S., Köfiler A., Behr G., Kataev V., Büchner B. *J. Exp. Theor. Phys.* **114**, 662 (2012)
14. Dengler E., Deisenhofer J., Krug von Nidda H.-A., Khim S., Kim J.S., Kim K.H., Casper F., Felser C., Loidl A. *Phys. Rev. B* **81**, 024406 (2010)
15. Ying J.J., Wu T., Zheng Q.J., He Y., Wu G., Li Q.J., Yan Y.J., Xie Y.L., Liu R.H., Wang X.F., Chen X.H. *Phys. Rev. B* **81**, 052503 (2010)
16. Pascher N., Deisenhofer J., Krug von Nidda H.-A., Hemmida M., Jeevan H.S., Gegenwart P., Loidl A. *Phys. Rev. B* **82**, 054525 (2010)
17. Garcia F.A., Leithe-Jasper A., Schnelle W., Nicklas M., Rosner H., Sichelschmidt J. *New J. Phys.* **14**, 063005 (2012)
18. Rosa P.F.S., Adriano C., Garitezi T.M., Ribeiro R.A., Fisk Z., Pagliuso P.G. *Phys. Rev. B* **86**, 094408 (2012)

19. Krug von Nidda H.-A., Kraus S., Schaile S., Dengler E., Pascher N., Hemmida M., Eom M.J., Kim J.S., Jeevan H.S., Gegenwart P., Deisenhofer J., Loidl A. *Phys. Rev. B* **86**, 094411 (2012)
20. Hemmida M., Krug von Nidda H.-A., Günther A., Loidl A., Leithe-Jasper A., Schnelle W., Rosner H., Sichelschmidt J. *Phys. Rev. B* **90**, 205105 (2014)
21. Chen X.H., Wu T., Wu G., Liu R.H., Chen H., Fang D.F. *Nature* **453**, 761(2008)
22. Klauss H.-H., Luetkens H., Klingeler R., Hess C., Litterst F.J., Kraken M., Korshunov M.M., Eremin I., Drechsler S.-L., Khasanov R., Amato A., Hamann-Borrero J., Leps N., Kondrat A., Behr G., Werner J., Büchner B. *Phys. Rev. Lett.* **101**, 077005 (2008)
23. Ren Z.A., Che G.-C., Dong X.-L., Yang J., Lu W., Yi W., Shen X.-L., Li Z.-C., Sun L.-L., Zhao F.Z.-X. *Europhys. Lett.* **83**, 17002 (2008)
24. Liu Y., Sun D.L., Park J.T., Lin C.T. *Physica C* **470**, S513 (2010)
25. Joshi J.P., Bhat S.V. *J. Magn. Reson.* **168**, 284 (2004)
26. Elliott R.J. *Phys. Rev.* **96**, 266 (1954)
27. Yafet Y. *Solid State Phys.* **14**, 1 (1963)
28. Wu T., Ying J.J., Wu G., Liu R.H., He Y., Chen H., Wang X.F., Xie Y.L., Yan Y.J., Chen X.H. *Phys. Rev. B* **79**, 115121 (2009)
29. Günther A., Deisenhofer J., Kant Ch., Krug von Nidda H.-A., Tsurkan V., Loidl A. *Supercond. Sci. Technol.* **24**, 045009 (2011)
30. Simon F., Dóra B., Murányi F., Jánossy A., Garaj S., Forró L., Bud'ko S., Petrovic C., Canfield P.C. *Phys. Rev. Lett.* **101**, 177003 (2008)